Naphthalene oxidation over 1%Pt and 5%Co/γ-Al_2O_3 catalysts: reaction intermediates and possible pathways

Xiao-Wen Zhang[a], Shou-Cang Shen[a], Kus Hidajat[a], Sibudjing Kawi[a], Liya E. Yu[a,*], and K.Y. Simon Ng[b]

[a]*Department of Chemical & Biomolecular Engineering, National University of Singapore, Singapore 119260, Singapore*
[b]*Department of Chemical Engineering and Material Science, Wayne State University, Detroit, MI 48202,USA*

Received 3 December 2003; accepted 27 April 2004

The decomposition, addition, and polymerization pathways of naphthalene oxidation over 1% Pt/γ-Al_2O_3 and 5% Co/γ-Al_2O_3 catalysts are discussed based on the relative concentration of intermediates found in this study along with a review of various reaction mechanisms. The identified intermediates were classified in three categories; (1) naphthalene-decomposed products, (2) naphthalene-derivatives, and (3) polymerized polycyclic aromatic compounds (PAC).

KEY WORDS: catalytic oxidation; naphthalene; catalysts; intermediate; reaction pathway.

1. Introduction

Substantial polycyclic aromatic compounds (PACs) have been found in diesel exhaust [1–5]. These are of special concern because PACs are among the most toxic pollutants [6–8], and can be transported by small particles deep into human lungs. Therefore, it is desired that new formulations of metal-based catalysts, which are effective in controlling NO_x problems, are also utilized to satisfactorily mitigate PACs toxicity in diesel emissions. A few metal catalysts were reported to efficiently decompose phenol [9], benzene and ethylbenzene [10], xylene [11], naphthalene [12–14], and PACs mixtures [15]. However, additional PAC by-products were found during the catalytic decomposition of PACs [11,16]. These by-products often originate from different stages of catalytic oxidation reactions. Since the toxicity of intermediates differs from that of their parent compounds, identifying these intermediates is necessary to assess the effectiveness of individual catalysts for minimizing harmful emissions. In addition, as an extension of previous work [17], this study intended to reconcile the disproportionate amount of CO_2 generated with the amount of decomposed reactant during the catalytic oxidation of naphthalene over Pt and Co supported catalyst.

The intermediates generated during naphthalene oxidation over Pt and Co catalysts were collected. Both gas-phase compounds and adsorbates on catalyst surfaces were analyzed to examine the effects of different reaction conditions. The data presented in this paper corroborate the findings that stronger chemisorption of naphthalene on the Pt catalyst results in more by-products [17], while a shorter residence time leads to more types of heavy PACs found on catalysts. To the best of our knowledge, this is the first study identifying the intermediates generated during catalytic oxidation of naphthalene over metal-supported catalysts. Based on the relative concentration of intermediates and free-radical measurements, reaction pathways of naphthalene oxidation over the Pt and Co catalysts are proposed. Further studies are needed to elucidate the relative importance of the suggested reaction pathways.

*To whom correspondence should be addressed.
E-mail: cheley@nus.edu.sg

2. Experimental description

2.1. Catalysts and reaction system

Among the noble and base metal catalysts studied [17], Pt and Co supported catalysts demonstrated the highest activities for oxidative decomposition of naphthalene. Therefore, the reactions over these two catalysts were selected for examining the intermediates formed at various reaction temperatures. Methods of catalyst preparation and reaction system used have been described elsewhere [17]. In brief, 1% Pt and 5% Co catalysts were prepared by co-impregnating the γ-Al_2O_3 support (Strem Chemicals, USA) with appropriate metal salt solutions before drying at 120 °C. Prior to catalytic oxidation, the Pt and Co supported catalysts were calcined for 4 h at 500 °C and 700 °C, respectively.

The reaction system consisted of a naphthalene source, a catalytic reactor, and an on-line detection system using gas chromatography coupled with a mass spectrum detector (GC-MS). The reactions were carried out using 150 mL/min gas mixture containing 10% oxygen and 90% helium. The reactant mixtures were calibrated and adjusted to ensure that the inlet

1011-372X/04/0700–0087/0

naphthalene containing a constant concentration of 100 ppm. About 0.5 g of catalyst was placed in the reactor tube and underwent reduction at 500 °C for 2 h before the reactant mixture was introduced. Two bubblers containing toluene were used alternately to continuously collect gas-phase hydrocarbons (such as un-reacted naphthalene) from the reactor outlet. The gas products emerging from the bubbler were then measured via an on-line GC-TCD (6890 series II, Hewlett-Packard, USA), equipped with three columns, a Porapak Q column (Hewlett-Packard, USA) for separating CO_2 and ethane, a molecular sieve column (Hewlett-Packard, USA) for separating N_2, O_2, and CO, and a DC-200 column (Hewlett-Packard, USA) for removing larger hydrocarbons to protect the other two columns.

The reaction temperatures in this study were selected according to the catalytic oxidation of naphthalene conducted at a steady state with a space velocity of 20,000 h^{-1}. Table 1 summarizes the naphthalene conversion and CO_2 yield as a function of reaction temperatures for both Pt and Co supported catalysts. The data were taken for 12 hours after the system reached steady state. The conditions displayed in table 1 represent various stages of intermediate formation, accounting for the difference between produced CO_2 and decomposed naphthalene, serving as a reference for selecting suitable reaction conditions to investigate the intermediates generated during the catalytic reactions of naphthalene. To assess the effects of residence time of reactants on intermediates adsorbed on the catalysts, catalytic oxidation of naphthalene was also conducted with 0.5 g of catalyst under a space velocity of 4000 h^{-1} by proportionally adjusting the flow rate of the carrier gas. The data were collected for 2 h after the system reached steady state.

Table 1
Catalytic oxidation of naphthalene under steady state at a space velocity of 20,000/h

Supported catalyst	Reaction temperatures (°C)	Naphthalene conversion[a] (%)	CO_2 yield[b] (%)
Pt catalyst	150	NA[c]	UD[d]
	200	72	UD[d]
	250	84	14
	275	87	72
	300	90	>90[e]
Co catalyst	300	<1	UD[d]
	350	33	6
	400	72	86

[a]Naphthalene conversion was measured based on bulk analysis of naphthalene collected at the outlet of the reactor every 15 min for the entire time-on-stream.
[b]CO_2 yield was obtained through on-line GC analysis.
[c]NA – not available.
[d]UD – under detection limit.
[e]The CO_2 yield higher than the naphthalene conversion could be due to different analysis approaches.

2.2. Intermediates collection

Gaseous intermediates were collected in bubblers containing around 8 μg (0.08 mL of 104.8 ìg/mL) of perdeuterated tetracosane-d_{50} ($C_{24}D_{50}$, Aldrich Chem. Co., USA) as an internal standard to monitor the operation loss throughout the procedure. The bubblers were placed in a liquid-nitrogen bath to instantaneously trap all gas-phase intermediates generated during reactions for 2 h. After removal from the liquid-nitrogen bath, 3 mL of dichloromethane (DCM, Merck, Germany) was introduced to wash the trapped compounds from the bubblers before concentrated to 0.2 mL utilizing a Reacti-Vap™ microconcentrator (Pierce, PIERCE Co., USA). To analyze the adsorbate on catalyst surfaces, the reactions were quenched before catalysts in the reactor were retrieved. About 3 mL of DCM was used to extract the compounds on used catalysts twice, followed by filtration to separate the extract from the catalysts. The extract was then concentrated to 0.2 mL prior to GC-MS injections. Pure catalysts, not subjected to the reaction, were extracted using the same procedure as a control to evaluate background interference, and no significant peak was found.

To identify the compounds containing oxygenated substituents, a 0.2 mL of the extract was withdrawn and dried with a mild nitrogen flow followed by adding a 40 μL of DCM and 10 μL of derivatization reagent, bis(trimethylsilyl)trifluoroacetamide (BSTFA, Sigma, USA). The GC-MS (6890 series II, Hewlett-Packard, USA) analysis was conducted after the derivatization took place for 20 min. All the derivatized extracts were analyzed via GC-MS coupled with an HP-5 column (Hewlett-Packard, USA). The oven temperature was programmed at 60 °C for 2 min, and then increased to 280 °C at a rate of 8 °C per minute. A 2 μL of 1-phenyldodecane (1-PD, Aldrich Chem. Co., USA) at 25.2 μg/mL was co-injected to account for the machine performance of GC-MS. Blank tests were conducted to measure the background compounds, which exhibited negligible response. In addition, to examine catalyst-bound radicals, the Pt catalyst utilized for naphthalene oxidation at 250 °C with a space velocity of 4000 hr^{-1} was examined by electron paramagnetic resonance (EPR) at room temperatures using a Bruker Elexsys E500 spectrometer (Bruker Biospin GMBH, Germany) coupled with double rectangular (TE102) cavity. The sample was weighed before underwent the quantification of spin concentration along with a strong pitch (0.11% in KCL) Bruker/Varian standard. The EPR spectra were acquired with a center field at 3481.95G and based on an average of 100 scans. Table 2 summarizes the individual analyses taken place in this study.

Table 2
Analyses of gaseous products and intermediates generated during the catalytic reactions of naphthalene

Components	Collection	Detection method
Gases (e.g., CO_2)	none	On-line GC-TCD
Gaseous hydrocarbons (e.g., un-reacted naphthalene)	Bubblers containing toluene	Off-line GC-FID
Gas-phase intermediates (e.g., benzaldehyde)	Cryo-trapping followed by DCM extraction	Off-line GC-MS
Intermediates (adsorbates) on catalysts (e.g., 1,1'-binaphthalene)	DCM extraction	Off-line GC-MS
Catalyst-bound free radicals	Catalysts	Off-line EPR

3. Results and discussion

3.1. Effects of reaction conditions

Table 3 displays the intermediates identified via GC-MS as a function of reaction temperature and space velocity. For a space velocity of 4000 h^{-1}, both gas-phase and adsorbate intermediates were collected at 130 °C and 250 °C for reactions over the Pt catalyst, while at 350 °C, 400 °C, and 450 °C over the Co catalyst. Most gas-phase products during the reactions at 20,000 h^{-1} were below detection limit, and thus only adsorbate concentrations are listed in table 3b. The intermediates identified in this study can be classified into three categories: (1) naphthalene-decomposed products, containing major fragments originated from naphthalene decomposition, (2) naphthalene derivatives, comprising alkyl and/or oxygenated substituents, and (3) polymerized PACs, including heavy PACs with and without oxygenated substituents. Compounds such as 2-cyclohexen-1-one and phthalic anhydride comprising fragments originating from naphthalene decomposition were classified under group (1) and were found in most of the samples collected from reactions with a space velocity of 4000 h^{-1}. Note that the compounds in group (1) could have molecular weight (MW) larger than naphthalene due to the addition of oxygenated and/or alkyl substituents. The oxygenated alkyl compounds, such as 1,4-butanediol, oxalic acid, and benzoic acid, were detected in trace amounts. The compound class of phthalate represents a variety of phthalic acid esters appeared in the GC-MS chromatograms. Although the

Table 3(a)
Intermediates during catalytic oxidation of naphthalene at a space velocity of 4000/hr

Compound	Pt Catalyst				Co Catalyst					
	Gas-phase (ppb)		Catalyst surface (μg/g catalyst)		Gas-phase (ppb)			Catalyst surface (μg/g catalyst)		
	130 °C	250 °C	130 °C	250 °C	350 °C	400 °C	450 °C	350 °C	400 °C	450 °C
Naphthalene-decomposed compounds										
Ethanediol			[b, f]					[d, f]	[d, f]	[d, f]
1,4-butanediol			[c, f]						[e, f]	[e, f]
Oxalic acid								[d, f]		
Propanoic acid, 2-methyl-, (1,1-dimethylethyl)-2-methyl-1,3-propanediyl ester	0.67[c]		0.25[a]	0.27[d]	1.57[d]	8.40[c]	0.77[d]	0.37[c]	0.08[c]	0.13[c]
2-cyclohexen-1-one	1.92[c]		0.03[b]	0.31[b]	1.48[c]	10.60[b]	3.74[b]	0.11[c]		
Benzaldehyde	1.83[a]					12.7[b]	1.19[b]	0.06[d]	0.15[a]	0.04[b]
Benzoic acid			[b, f]					[b, f]		
Phthalic anhydride	2.34[a]			0.13[b]	1.77[a]	1.45[a]				
Phthalate[g]	6.82–9.59	0.45–0.79	0.06–4.68	0.07–5.9	11.5–14.4	37.5–65.9	6.29–9.82	0.10–0.57	0.03–0.81	0.01–0.23
Naphthalene derivatives										
Naphthalene, 1-methyl	1.03[b]		3.91[a]							
Naphthalene, 2-methyl	1.76[b]		1.18[a]							
Naphthalene, 2-ethyl			0.18[b]							
Naphthalenol			1.22[a]							
Naphthalenemethanol			0.17[b]							
1,4-naphthalenedione			0.34[a]							
2-naphthalene-carboxaldehyde			3.10[a]							
1,1'-binaphthalene			0.23[a]							
1,2'-binaphthalene			4.61[a]							
2,2'-binaphthalene			15.76[a]							
Polymerized-Oxygenated PACs										
7H-benz[de]anthracen-7-one			0.12[c]							
5,12-naphthacenedione			0.05[c]							

Table 3(b)
Intermediates during catalytic oxidation of naphthalene at a space velocity of 20,000/hr

Compound	Pt Catalyst surface (μg/g catalyst)					Co Catalyst surface (μg/g catalyst)		
	150 °	200 °	250 °	275 °	300 °	300 °	350 °	400 °
Naphthalene-decomposed compounds								
Benzoic Acid							3.26[a]	
Propanoic acid ester						0.37[c]		
Propanoic acid, 2-methyl-, 1-(1,1-dimethylethyl)-2 -methyl-1,3-propanediyl ester								
Phthalates[g]	2.8[c]	7.02[d]	3.55[d]	9.68[e]	11.94[c]	1.07[c]	0.62[d]	0.29[e]
Naphthalene derivatives								
Naphthalene, 1-methyl		3.26[c]		2.14[a]				0.07[c]
1,2′-binapthelene		1.28[c]						
2,2′-binaphthalene				34.9[a]				
Polymerized-Oxygenated PACs								
7H-benz[de]anthracen-7-one						1.34[a]		
Benz[a]anthracene-7,12-dione				2.85[b]				
Polymerized PAHs								
Benzo[ghi]fluoranthene				1.31[b]				
Benzo[e]pyrene				27.6[a]				
Triphenylene				0.83[a]				

[a]With library mass spectrum match higher than 90%.
[b]With library mass spectrum match between 80–90%.
[c]With library mass spectrum match higher than 70–80%.
[d]With library mass spectrum match higher than 60–70%.
[e]With library mass spectrum match lower than 60%.
[f]Oxygenated compounds: only qualitative identification is available.
[g]Represent various phthalic acid esters.
[h]The listed concentrations can correspond to a solvent extract concentration of a few hundred ppb measured via GC-MS.

ester groups of the phthalate varied, they were recognized based on consistent elution time and substantial mass fragments of 149 and 167. Hence, table 3 displays a concentration range to represent all the compounds comprising phthalate components.

The fact that both naphthalene-derivatives and heavy PAC classes were detected suggests that naphthalene functioned as a basic building block for high MW intermediates. Naphthalene derivatives, including dimerized PAC compounds, contained alkyl and/or oxygenated substituents and had no more than two condensed aromatic rings. Heavy PAC compounds are referred to the ones resulting from naphthalene polymerization, consisting of multiple aromatic rings and/or oxygenated components.

More intermediate species were detected from reactions conducted at the space velocity of 4000 h^{-1} (table 3a) than those of 20,000 h^{-1} (table 3b), suggesting that longer residence time allowed various decompositions to take place over both the Pt and Co catalysts. On the other hand, peri-condensed PAH (such as benzo[ghi]fluoranthene) on catalysts only occurred at the space velocity of 20,000 h^{-1}. This suggests that with shorter reaction time naphthalene tended to undergo polymerization prior to direct decomposition. The polymerized PACs may serve as precursors to the resultant oxidation products, such as phthalate compounds. More naphthalene-derivatives found over the Pt catalyst at 130 °C (table 3a) seemed also to support the idea that adsorbed naphthalene inclined to undergo growth processes before fragmentation.

At reaction temperature of 130 °C (table 3a), various higher MW compounds (such as naphthalenol and 7H-benz[*de*]anthracen-7-one) were extracted from the Pt catalyst surface compared to the gas-phase compounds captured in the bubblers. This indicates that most naphthalene-decomposition reactions were catalytic and occurred over Pt catalyst surface rather than in the gas-phase. At 250 °C and a space velocity of 4000 h^{-1}, negligible amount of intermediate could be detected in the bubblers and few heavy compounds were recovered from the Pt catalyst. This agrees with the previous observation, based on the trend of CO_2 produced, that most naphthalene was converted to final oxidation products by 275 °C [17].

The identified intermediate products correlate well with previously reported findings [17] regarding the effects of chemisorption of naphthalene on Pt catalyst versus Co catalyst. Unlike the intermediates found during naphthalene oxidation on the Pt catalyst, fewer intermediates were detected over the Co catalyst, particularly at 4000 h^{-1}. It is interesting to note that the gas-phase intermediates and adsorbates on the Co catalyst appeared similar at all three temperatures,

350 °C, 400 °C, and 450 °C (table 3a). In addition, most of the intermediates appeared to originate from naphthalene decomposition. The different intermediates found on Pt- versus Co-catalyst suggest that more direct decomposition and less polymerization of naphthalene occurred over the Co catalyst. Badini et al. [10] reported that the bonding of naphthalene on the Co catalyst was much weaker than on the Pt catalyst. This led to the postulation that the weaker interactions between naphthalene and the Co surface allowed the ring structures to be quickly ruptured [17]. In addition, since the 1%Pt/γ-Al_2O_3 catalyst might have less surface coverage over the support compared to the 5%Co/γ-Al_2O_3, more hydroxyl groups could be available on the Pt catalyst to adsorb naphthalene and intermediates. Hence, it is not surprising that, relative to the Pt catalyst, the Co catalyst retained fewer intermediates, and appeared to be insensitive to the change in space velocity. Furthermore, the more direct and complete conversion of naphthalene on the Co catalyst explains the good agreement between the amount of CO_2 produced from the catalytic oxidation and the amount of naphthalene-decomposed [17]. On the other hand, the relatively strong chemisorption of naphthalene on the Pt catalyst apparently promoted naphthalene to participate in further reactions and resulted in more intermediate byproducts (see table 3).

It is important to note that heavy PACs produced during the catalytic oxidation of naphthalene can potentially increase the toxicity of diesel exhaust. In addition to being more persistent under severe thermal conditions and in exhausts [18,19], the 4- and 5-ring PAHs were found to be much more carcinogenic because of the bay-region structure [18,20], which may pose more serious health concerns. Since PACs consisting of more than two condensed aromatic rings were not found in the gas-phase, PAC polymerization occurred primarily on catalyst surface. Fortunately, at reaction temperatures above 300 °C, all the PACs formed were completely decomposed through subsequent reactions occurring over Pt catalyst surface.

3.2. Possible reaction pathways

The concentrations and chemical compositions of the identified intermediates suggest that catalytic oxidation of naphthalene mainly involved decomposition, addition, and polymerization pathways. However, in addition to the typical electrophilic and nucleophilic mechanisms, gas-phase free-radical reactions can be part of the overall reaction scheme. Furthermore, since a homogeneous model was successfully coupled to heterogeneous reactions [21], the scenario that naphthalene might follow homogeneous reaction pathways during catalytic oxidation is also considered. The following discussion is a review of different decomposition, addition and polymerization pathways proposed for naphthalene oxidation. An attempt was then made to postulate formation pathways of the phthalates found in this study.

3.3. Decomposition pathways

Employing the reaction pathways during selective gas-phase catalytic oxidation of naphthalene has been reported [22,23]. Figure 1 shows that 1,4-naphthalenedione was produced over vanadium oxide-based catalysts without requiring naphthalene undergo ring destruction by following route (a), while phthalic anhydride was subsequently produced with ring rupture [23]. Alternatively, as pathway (b) in figure 1

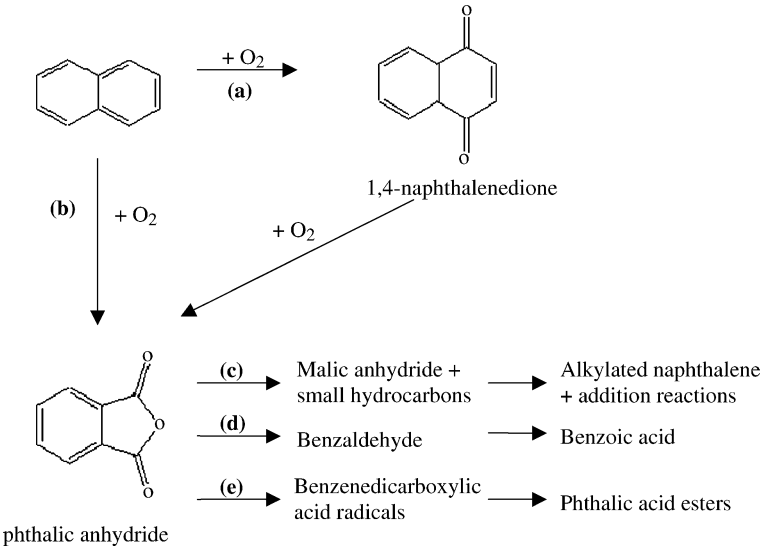

Figure 1. Possible pathways of formation of various phthalates during naphthalene catalytic oxidation (according to Brückner and Baerns (1997), and Linstromberg and Baumgarten (1983)).

shows, Linstromberg and Baumgarten [22] reported that naphthalene could be directly oxidized to phthalic anhydride during oxidation over vanadium pentoxide catalyst, and can be easily converted to phthalic acid ester. The presence of both 1,4-naphthalenedione and phthalic anhydride among the samples analyzed indicates that both pathways could contribute to the phthalates formed in this study. However, the more frequent occurrence and higher concentration of phthalic anhydride given in table 3 suggest that route (b) was a more favorable pathway for the initial naphthalene-decomposition. It is interesting to note that phthalates were produced over both catalysts at all reaction temperatures and space velocities studied. Thus, in addition to phthalate compounds produced by plasticizer industries, emissions due to incomplete engine combustion may contribute to the phthalates measured in the atmosphere.

Following the initial oxidation of naphthalene, phthalic anhydride could undergo different reactions forming various intermediates. Under a non-selective oxidation process, Brückner and Baerns [23] reported that phthalic anhydride could be converted to malic anhydride, and the smaller hydrocarbon fragments generated during the process could contribute to producing compounds such as methylated naphthalene and triphenylene (route (c) in figure 1). Phthalic anhydride could also be oxidized to benzaldehyde (route (d)), to be further oxidized to benzoic acid with the presence of oxygen and at temperatures above 300 K [24]. Methylated naphthalene found during naphthalene oxidation over the Pt catalyst (130°C at 4000 h^{-1}) appeared to be much more prominent than benzaldehyde and benzoic acid (table 3a), indicating that phthalic anhydride inclined to follow reaction pathway (c) involving malic anhydride to facilitate the formation of alkylated naphthalene at the early stage of oxidation over the Pt catalyst.

Comparable to the concentration of methylated naphthalene, the substantial amount of phthalic acid esters indicates the different reactions which phthalic anhydride participated in. In liquid phase, phthalic anhydride could undertake a radical mechanism to form benzenedicarboxylic-acid radicals, which are important precursors to producing phthalic acid esters [24]. With the ring opening and decomposition of naphthalene, the freed alkyl chain groups could be available to attach to the benzenedicarboxylic-acid radicals forming various esters observed in this study. Since the hydrocarbon fragments formed through the reaction route (c) in figure 1 may form the ester functional groups during the radical reaction mechanisms (route (e)), both routes (c) and (e) may play important roles of determining the fate of phthalic anhydride during naphthalene oxidation over the Pt and Co catalyst.

Table 3a shows that, with the same space velocity, the concentrations of some of the phthalic acid esters extracted from the Pt catalyst were more than 4 μg per gm of catalyst at two reaction temperatures (130 °C and 250 °C), while the total amounts of phthalates from the Co catalyst were no more than 1 μg per gm of catalyst at all three reaction temperatures (350 °C, 400 °C, and 450 °C). The weaker interactions with the Co catalyst may allow the second ring of naphthalene to be quickly broken following the rupture of the first ring. Therefore, less phthalate found on the Co catalyst further supports the notion that the Co catalyst tended to completely decompose naphthalene with fewer by-products.

3.4. Addition pathways – Alkylation of naphthalene

The addition mechanisms during naphthalene oxidation over Pt and Co catalyst involved the attachment of alkyl substituents and combination of aromatic compounds (such as dimerization), while polymerization contributed to the heavily condensed PACs. Because methylnaphthalene was most commonly found on the Pt catalyst at a space velocity of 4,000 h^{-1} (table 3a), figure 2 presents the possible alkylation pathways of methylnaphthalene as an example based on respective cationic-intermediate formation and free-radical formation. The presence of methane/methyl components could account for the small hydrocarbon fragments generated through the route (c) shown in figure 1, as explained in the previous section. Linstromberg and Baumgarten [22] reported that naphthalene followed the similar pathways undertaken by benzene during selec-

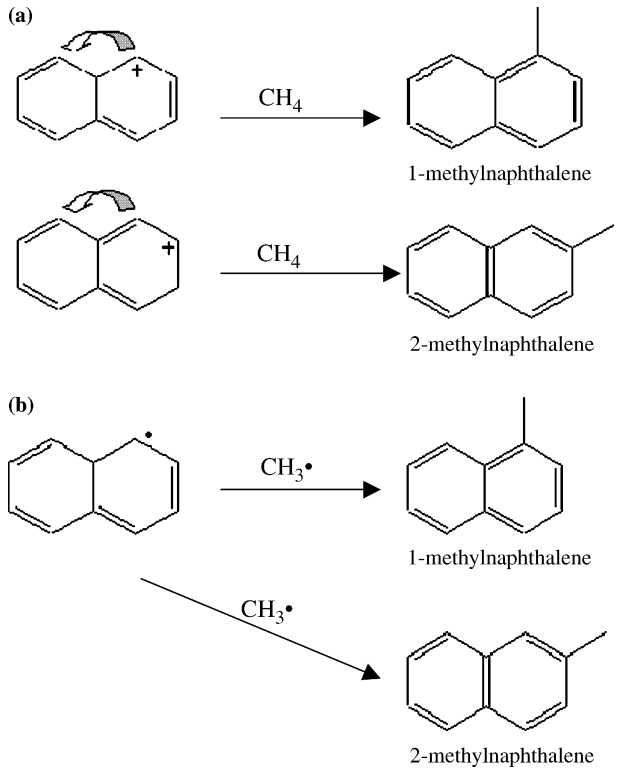

Figure 2. Potential methylation pathways for methylnaphthalene.

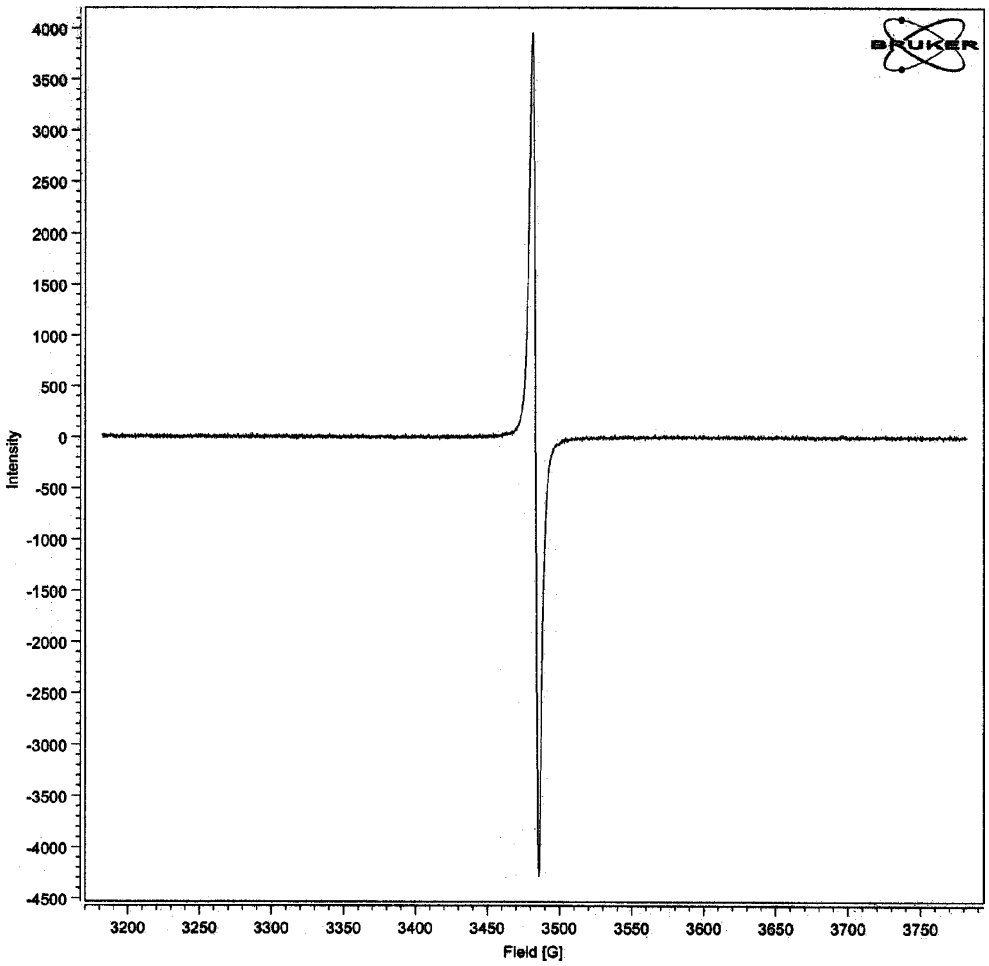

Figure 3. EPR spectrum of free radicals on the Pt catalyst under 250 °C and 4000 h^{-1}.

tive gas-phase oxidation, in particular favoring the alkylation on the α-position. While naphthalene cationic intermediate might react with methane to form methylnaphthalene, methylated naphthalene were found on the Pt catalyst, rather than among the gas-phase products collected during the catalytic oxidation in this study.

In addition to forming ionic intermediates, naphthalene may directly react with methyl radicals available during the oxidation over the Pt catalyst. Methyl radicals have been found during deNO_x reactions over various catalysts [25–27]. The radicals, which were generated on catalyst surface, triggered gas-phase reactions forming reactive intermediates followed by heterogeneous transformation [21]. In addition, our EPR spectrum (figure 3) shows that the free-radicals on the Pt catalyst at reaction temperature of 250 °C and 4,000 h^{-1} exhibited a concentration of 2.51×10^{18} spins per gram of the Pt catalyst, and contained a *g*-value between 2.0026 and 2.0028 corresponding to 1- to 5-ring aromatic radicals [28]. This indicates that radical reactions (route (b)) in figure 2 could contribute to the presence of methylated naphthalene on Pt catalyst. In addition, free-radical reactions involving naphthalene have also been reported during a catalytic oxidation process [11]. Hence, the various methylnaphthalene extracted from the Pt catalyst surface could be formed through the reactions between naphthalene radicals and methyl radicals. Similarly, it is expected that other alkylated compounds, such as ethylnaphthalene, can be found over the Pt catalyst during the catalytic oxidation of naphthalene. In spite of ionic or radical reactions, under continuous oxidative conditions, alkylated compounds could subsequently undergo further oxidation to produce compounds containing oxygenated substituents, such as naphthalenol and 2-naphthalene carboxaldehyde found on Pt catalyst surface at 130 °C (table 3a).

3.5. Addition pathways – Dimerization of naphthalene

While investigations of PACs formation during benzene and xylene oxidation were conducted by Guisnet *et al.* [11] and by Becker and Förster [16], little research work has attempted to identify the heavy by-products formed during catalytic oxidation of naphthalene under high concentrations of oxygen. Since naphthalene and benzene have aromatic structures and can form a cationic-intermediate [22], the mechanisms used for PAC formation during benzene and xylene

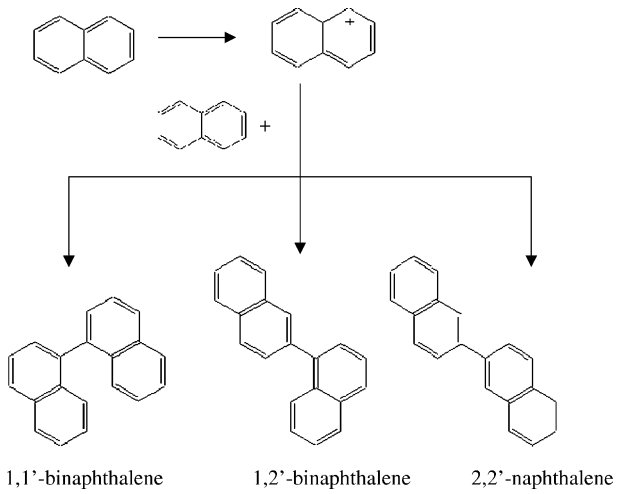

Figure 4. Potential cationic intermediate pathway of dimerization of naphthalene.

oxidation may explain one of the possible pathways to forming larger PACs during naphthalene decomposition. Following the ionic-addition pathway during benzene oxidation over Pd and Cu zeolite catalysts in the gas phase [16], figure 4 displays possible cationic reactions forming binaphthalene isomers presented in this study. Note that dimerization occurring through radicals reactions was reported under pyrolysis conditions at around 1000 °C with a residence time of about 0.7 second [29], and pyrene radicals were also found to contribute to bi-pyrene during the oxidation of xylene over 0.2% Pd-zeolite catalysts [11]. While further investigation is needed to compare the dominance of ionic versus radical reactions, our EPR result (figure 3) showing the presence of 1- to 5-ring free aromatic radicals on the Pt catalyst supports that biaryl radical linkages could contribute to binaphthalene isomers on the surface of catalysts.

3.6. Polymerization of oxygenated PACs

Based on various infrared and GC-MS studies, larger oxygenated PACs – anthraquinone and benzophenone – measured during gas-phase xylene oxidation over a 0.2% Pd/HFAU catalyst [11] were also found during the deep oxidation of benzene over Pd and Cu exchanged Y-type zeolite catalysts [16]. During benzene oxidation, Becker and Förster [16] further demonstrated that larger PACs, which were formed through benzene-participating polymerization, underwent subsequent oxidation to form anthraquinone before further oxidizing to 1,4-naphthalenedione and phthalic anhydride. By undertaking benzene addition and carboxylic acid replacement, phthalic anhydride was converted to benzoylbenzoic acid, an intermediate serving as a precursor either leading back to anthraquinone, or eventually resulting in new compounds, xanthone and fluorenone [16]. Since catalytic oxidation mechanisms proposed for benzene and xylene have been used to successfully explain naphthalene oxidation under similar conditions [22], figure 5 portrays our attempt to show one potential mechanism forming the intermediates produced during naphthalene oxidation over the Pt catalyst. Similarly, phthalic anhydride measured in this study could have naphthalene addition to form keto acids as the intermediates a, b, and c shown in figure 5. By following the decarboxylation pathway, the oxygenated large PACs 7H-benz[de]anthracen-7-one, benz[a]anthracene-7-12-dione, and 5,12-naphthacenedione could be formed on Pt catalyst at 130 °C (4000 h^{-1}) and 275 °C (20,000 h^{-1}). Since phthalic anhydride appeared to be the key compound for forming the abundant phthalates adsorbed on the catalysts, as discussed earlier (figure 1), less phthalic anhydride would be available to undergo the polymerization reactions forming larger oxygenated PAC. Hence, the reaction pathways forming larger oxygenated keto acids were expected to be relatively less favorable during a more severe (higher reaction temperature) catalytic oxidation of naphthalene.

3.7. Polymerization of PAH

The last group of condensed PAHs (benzo[*e*]pyrene, triphenylene, and benzo[*ghi*]fluoranthene) found on the Pt catalysts at 20,000 h^{-1} suggests that naphthalene underwent polymerization to form PAHs composed of more condensed aromatic rings. According to the oxidation conditions and the presence of phthalic anhydride as well as larger oxidized PAC compounds, the heavy condensed PACs containing more aromatic rings could be resulted from the reaction of anhydrides, involving condensation, dehydrogenation, and/or cyclization of chain compound as proposed by Guisnet *et al.* [11]. Richter and Howard [30] and Ledesma *et al.* [31] suggested a free-radical pathway forming highly condensed PACs by the addition of C_2H_2 radicals to benzene or naphthalene radicals, which was eventually terminated by ring closure resulting in larger PACs. Since triphenylene and benzo[*ghi*]fluoranthene were reported during pyrolysis of coal and wood (above 800 °C with around 0.7 s of residence time in the reactor) [29], the proposed radical formation pathways could occur during naphthalene oxidation over catalysts with a space velocity of 20,000 h^{-1}. Although the polymerization forming condensed PACs did not appear as a prominent mechanism relative to others discussed previously, it further explains why almost 90% of naphthalene was converted at 275 °C yet a disproportionate amount of carbon dioxide was formed during the oxidation over the Pt catalyst. Since aromatic compounds can be the precursors of soot, this finding suggests that satisfactory catalysts should be capable of decomposing or suppressing the formation of polymerized aromatic compounds to reduce the amount of particles in diesel exhausts.

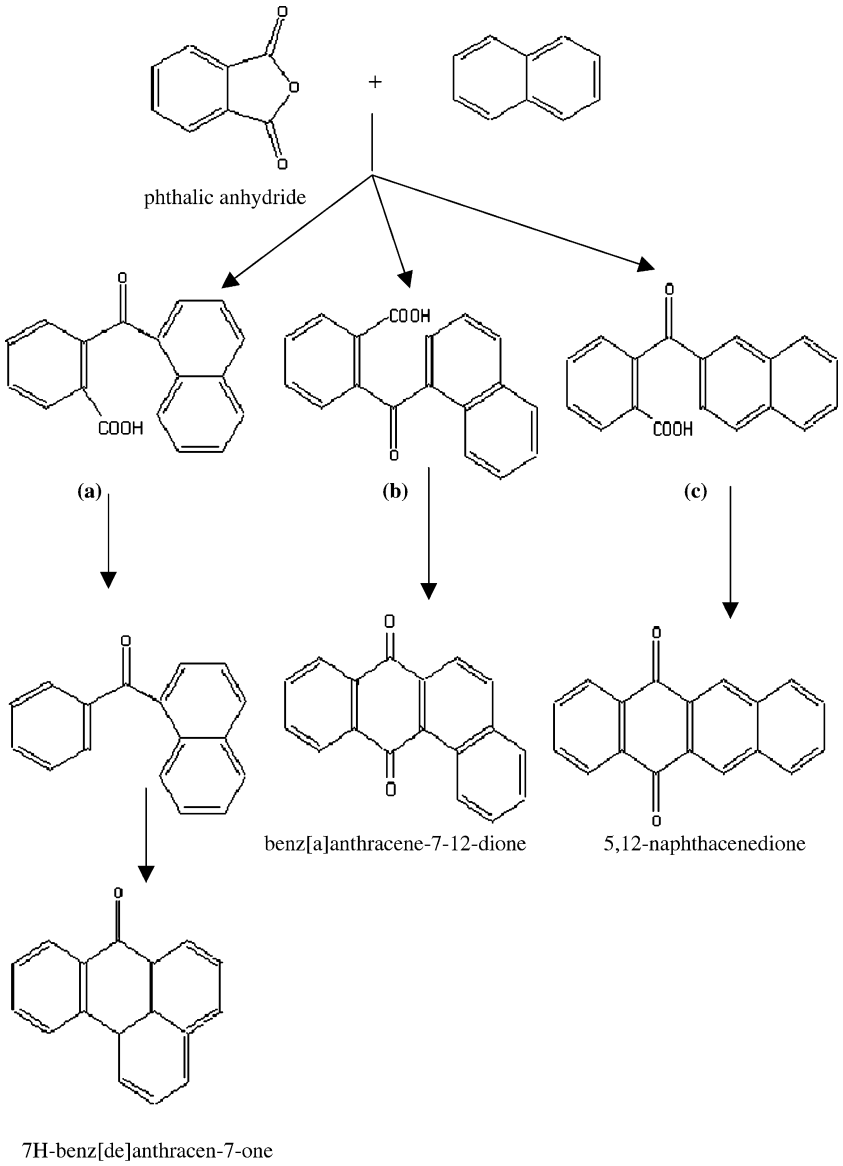

Figure 5. Possible formation pathways of heavy by-products during naphthalene oxidation.

4. Conclusions

The intermediates generated during catalytic oxidation of naphthalene over the 1%Pt/γ-Al_2O_3 and 5%Co/γ-Al_2O_3 catalysts were identified and classified as naphthalene-decomposed by-products, naphthalene derivatives, and polymerized PACs. The total concentration of gas-phase intermediates was less than 100 ppb. More intermediates were found during the catalytic oxidation of naphthalene over Pt catalyst than over Co catalyst. This suggests that naphthalene oxidation over Co catalyst involved less complex pathways, supporting the hypothesis that weaker adsorption of naphthalene on Co catalyst allowed more direct and complete oxidation of naphthalene. For catalytic oxidations spanning over a wide range of reaction temperatures, the chemical compositions of intermediates is important for designing more environmental-friendly catalysts.

Three classes of intermediates were identified: (1) naphthalene-decomposed compounds, (2) naphthalene derivatives, and (3) heavy PACs. Based on the relative concentrations of intermediates found in this study and a review of various reaction pathways, the following pathways are proposed:

1. The naphthalene-decomposed intermediates were mainly formed by forming phthalic anhydride followed by esterification, in addition to other oxidation processes;
2. Methylation and dimerization were the major mechanisms contributing to the presence of various naphthalene derivatives; and
3. The presence of the heavy PACs suggests that naphthalene underwent initial growth before decomposition during the catalytic naphthalene oxidation.

The derived reaction pathways can facilitate the evaluation of possible organic by-products in emissions for providing effective control of the toxicity of diesel exhausts.

Acknowledgment

The authors thank Dr. Yuri Kostetski for the free-radical measurements using EPR. Financial support provided by the National University of Singapore (Grant No. R-279-000-093-112) is gratefully acknowledged.

References

[1] H. Li, C.D. Banner, G.G. Mason, R. Westerholm and J.J. Rafter, Atmos. Environ. 30 (1996) 3537.
[2] H.H. Yang, W. Lee, H.H. Mi and C. Wang, Environ. Int. 24 (1998) 389.
[3] Z. Wang, M. Fingas, Y.Y. Shu, L. Sigouin, M. Landriault and P. Lambert, Environ. Sci. Technol. 33 (1999) 3100.
[4] P. Fleurat-Lessard, K. Pointet and M.F. Renou-Gonnord, J. Chem. Educ. 76 (1999) 962.
[5] D.S. Douce, M.R. Clench, M. Cooke and J. Wang, J. Chromatogr. A 786 (1997) 275.
[6] M.S. Zedeck, J. Environ. Pathology Toxicol. 3 (1980) 537.
[7] P.P. Fu and D. Herreno-Saenz, Environ. Carcin. Eco. Revs. C 17 (1999) 1.
[8] K. Nauss, Diesel Exhaust: A Critical Analysis of Emissions, Exposure and Health Effects. Summary of A Health Effects Institue (HEI) Special Report, HEI Diesel Working Group 1997.
[9] M.A. Walsh and J.R. Katzer, Ind. Eng. Chem. Process Design Develop. 12 (1973) 477.
[10] C. Badini, G. Saracco, V. Serra and V. Specchia, Appl. Catal. B 18 (1998) 137.
[11] M. Guisnet, P. Dege and P. Magnoux, Appl. Catal. B 20 (1999) 1.
[12] J. Carnö, M. Berg and S. Järås, Fuel 75 (1996) 959.
[13] A.K. Neyestanaki and L.-E. Lindfors, Fuel 77 (1998) 1727.
[14] A.K. Neyestanaki, L.-E. Lindfors, T. Ollonqvist and J. Vayrynen, Appl. Catal. A 196 (2000) 233.
[15] R. Weber, T. Sakurai and H. Hagenmaier, Appl. Catal. B 20 (1999) 249.
[16] L. Becker and H. Förster, Appl. Catal. A 153 (1997) 31.
[17] X.-W. Zhang, S.C. Shen, S. Kawi, K. Hidajat, L.E. Yu and K.Y.S. Ng, Appl. Catal. A 250 (2003) 341.
[18] M.J. Wornat, A.F. Sarofim, J.P. Longwell and A.L. Lafleur, Energy Fuels 2 (1988) 775.
[19] L.E. Yu, L.M. Hildemann and S. Niksa, Energy Fuels 12 (1998) 450.
[20] C.H. Ho, B.R. Clark, M.R. Guerin, B.D. Barkenbus, T.K. Rao and J.L. Epler, Mutat. Res. 85 (1981) 335.
[21] M.D. Fokema and J.Y. Ying, J. Catal. 192 (2000) 54.
[22] W.W. Linstromberg and H.E. Baumgarten, *Organic Chemistry* (D. C. Health and Company, Toronto, 1983) pp. 117–143.
[23] A. Brückner and M. Baerns, Appl. Catal. A 157 (1997) 311.
[24] R.G. Harvey, *Polycyclic Aromatic Hydrocarbons* (Wiley-VCH, New York, 1997) pp. 156–256.
[25] J. Vassallo, E. Miro and J. Petunchi, Appl. Catal. B 7 (1995) 65.
[26] K. Otsuka, Q. Zhang, I. Yamanaka, H. Tono, M. Hatano and H. Kinoshita, Bull. Chem. Soc. Jpn. 69 (1996) 3367.
[27] M.A. Vannice, A.B. Walters and X. Zhang, J. Catal. 159 (1996) 119.
[28] L. Petrakis and D.W. Grandy, *Free Radicals in Coals and Synthetic Fuels* (Elsevier, New York, 1983) p. 51.
[29] A.F. Sarofim, J.P. Longwell, M.J. Wornat and J. Mukherjee, in: *Soot Formation in Combustion: Mechanisms and Models*, ed. H. Bockhorn (Springer-Verlag, Berlin, 1994) pp. 485–496.
[30] H. Richter and J.B. Howard, Prog. in Energy Combust. Sci. 26 (2000) 565.
[31] E.B. Ledesma, M.A. Kalish and M.J. Wornat, Energy Fuels 13 (1999) 1167.